Effect of Solvation on the Rotation of Hydroxymethyl Groups in Carbohydrates

Glen D. Rockwell and T. Bruce Grindley*

Contribution from the Department of Chemistry, Dalhousie University, Halifax, NS B3H 4J3, Canada

Received June 4, 1998. Revised Manuscript Received August 25, 1998

Abstract: The solvent dependences of the populations of the hydroxymethyl rotamers of methyl 2,3,4,6-tetra-*O*-[$^2H_3$]-α-D-glucopyranoside (**2a**) and methyl 2,3,4-tri-*O*-[$^2H_3$]-α-D-glucopyranoside (**6**) in 10 and 8 solvents, respectively, have been determined by analysis of $^3J_{H5,H6R}$ and $^3J_{H5,H6S}$ values and by consideration of evidence for hydrogen bonding through infrared spectroscopy and $^3J_{H,OH}$ values. The methods used to determine coupling constants in individual hydroxymethyl rotamers were reexamined, and an improved protocol was developed. When O-6 is methylated (**2a**), the populations of the hydroxymethyl rotamers are largely independent of solvent polarity at ratios of about 61:38:0 *gg*:*gt*:*tg*, except that a small population (<4%) of the *tg* rotamer appears in the most polar solvents at the expense of the *gg* rotamer. When O-6 is unsubstituted (**6**), there are substantial changes in rotamer population as solvent polarity increases due to loss of intramolecular hydrogen bonding and stabilization of the more polar rotamers. The rotamer populations for **6** return to those adopted by the permethylated derivative (**2a**) in the most polar solvents. It was concluded that hydrogen bond donation from OH-6 to water is not important in determining hydroxymethyl rotational preferences. The well-known "reversed" chemical shift order of the two C6 protons of peracetylated glucopyranose derivatives was shown to also occur for permethylated derivatives and is ascribed to solvent effects in addition to anisotropy. The solvent effect on the chemical shift difference is attributed to the fact that one of the two protons stays on the same side of the pyranose ring in the two more populated rotamers while the other proton exchanges environments.

Introduction

Many biological recognition processes involve oligosaccharides attached to cell surfaces. The selectivities of these processes depend on the structure and the conformation of the carbohydrate molecules. One of the most important aspects of carbohydrate shape is the conformation about the exocyclic C5−C6 bond in hexopyranoses and pyranoses that have more than six carbon atoms. This feature is critical for the shapes of oligosaccharides or polysaccharides that contain (1→6) linkages or linkages to O7 or O8 of higher carbon sugars, such as sialic acid, but is also an important feature in sugars where O6 is unsubstituted. Although this aspect of carbohydrate conformation has been much studied by both theoretical and experimental methods,[1−24] there are still considerable uncertainties about the positions of the equilibria and, more importantly, the dominant factors in the determination of these positions.

The potential energy surface for rotation about the C5−C6 bond in D-aldohexopyranosides contains three minima that lie at roughly staggered orientations, commonly termed the *gg*, *gt*, and *tg* rotamers, where *g* stands for gauche and *t* stands for trans. The first letter in these labels refers to the torsional

(1) Barrows, S. E.; Storer, J. W.; Cramer, C. J.; French, A. D.; Truhlar, D. G. *J. Comput. Chem.* **1998**, *19*, 1111−1129.
(2) Bock, K.; Duus, J. Ø. *J. Carbohydr. Chem.* **1994**, *13*, 513−543.
(3) Nishida, Y.; Hori, H.; Ohrui, H.; Meguro, H. *J. Carbohydr. Chem.* **1988**, *7*, 239−250.
(4) (a) Ohrui, H.; Nishida, Y.; Watanabe, M.; Hori, H.; Meguro, H. *Tetrahedron Lett.* **1985**, *26*, 3251−3254. (b) Nishida, Y.; Ohrui, H.; Meguro, H. *Tetrahedron Lett.* **1984**, *25*, 1575−1578.
(5) (a) Morales, E. Q.; Padrón, J. I.; Trujillo, M.; Vázquez, J. T. *J. Org. Chem.* **1995**, *60*, 2537−2548. (b) Padrón, J. I.; Vázquez, J. T. *Chirality* **1997**, *9*, 626−637.
(6) (a) de Vries, N. K.; Buck, H. M. *Rec. Trav. Chim. Pays-Bas* **1987**, *106*, 453−460. (b) de Vries, N. K.; Buck, H. M. *Carbohydr. Res.* **1987**, *165*, 1−16.
(7) Hori, H.; Nishida, Y.; Ohrui, H.; Meguro, H.; Uzawa, J. *Tetrahedron Lett.* **1988**, *29*, 4457−4460.
(8) Nishida, Y.; Hori, H.; Ohrui, H.; Meguro, H.; Uzawa, J. *Tetrahedron Lett.* **1988**, *29*, 4461−4464.
(9) Streefkerk, D. G.; Stephen, A. M. *Carbohydr. Res.* **1976**, *49*, 13−25.
(10) Streefkerk, D. G.; de Bie, M. J. A.; Vliegenthart, J. F. G. *Tetrahedron* **1973**, *29*, 833−844.
(11) De Bruyn, A.; Anteunis, M. *Carbohydr. Res.* **1976**, *47*, 311−314.
(12) Ohrui, H.; Nishida, Y.; Higuchi, H.; Hori, H.; Meguro, H. *Can. J. Chem.* **1987**, *65*, 1145−1153.
(13) Wiesler, W. T.; Vázquez, J. T.; Nakanishi, K. *J. Am. Chem. Soc.* **1987**, *109*, 5586−5592.
(14) Jiménez-Barbero, J.; Junquera, E.; Martín-Pastor, M.; Sharma, S.; Vicent, C.; Penadés, S. *J. Am. Chem. Soc.* **1995**, *117*, 11198−11204.
(15) Abraham, R. J.; Chambers, E. J.; Thomas, W. A. *Carbohydr. Res.* **1992**, *226*, C1−C5.
(16) (a) Paulsen, H.; Peters, T.; Sinnwell, V.; Heume, M.; Meyer, B. *Carbohydr. Res.* **1986**, *156*, 87−106. (b) Brisson, J. R.; Carver, J. P. *Biochemistry* **1983**, *22*, 3680−3686.
(17) Hori, H.; Nishida, Y.; Ohrui, H.; Meguro, H. *J. Carbohydr. Chem.* **1990**, *9*, 601−618.
(18) Nishida, Y.; Hori, H.; Ohrui, H.; Meguro, H. *Agric. Biol. Chem.* **1988**, *52*, 887−889.
(19) Nishida, Y.; Hori, H.; Ohrui, H.; MeguIn Filero, H.; Zushi, S.; Uzawa, J.; Ogawa, T. *Agric. Biol. Chem.* **1988**, *52*, 1003−1011.
(20) Bock, K.; Pedersen, H. *Acta Chem. Scand., Ser. B* **1988**, *42*, 190−195.
(21) Bock, K.; Refn, S. *Acta Chem. Scand., Ser. B* **1987**, *41*, 469−472.
(22) Damm, W.; Frontera, A.; Tirado-Rives, J.; Jorgenson, W. L. *J. Comput. Chem.* **1996**, *17*, 1955−1970.
(23) Jansson, P.-E.; Kenne, L.; Kolare, I. *Carbohydr. Res.* **1994**, *257*, 163−174.
(24) (a) Engelsen, S. B.; Rasmussen, K. *J. Carbohydr. Chem.* **1997**, *16*, 773−788. (b) Engelsen, S. B.; Pérez, S.; Braccini, I.; Hervé du Penhoat, C. *J. Comput. Chem.* **1995**, *16*, 1096−1119.

10.1021/ja981958l CCC: $15.00
Published on Web 10/10/1998

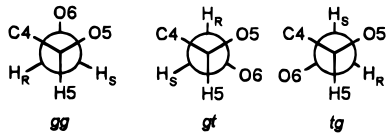

Figure 1. Nomenclature for C5−C6 rotamers.

relationship between O6 and O5, while the second letter refers to the relationship between O6 and C4 (see Figure 1).

Many factors have been considered to influence the C5−C6 rotameric populations, including 1,3-synaxial interactions, the gauche effect, anomeric configuration, hydrogen bonding, and solvent effects.[2] For galactopyranose derivatives, significant solvent effects have been observed,[6] but surprisingly, the effects of solvents on rotamer populations of glucopyranose derivatives have not been systematically studied experimentally. Extensive theoretical effort has been devoted to understanding the factors that influence hydroxymethyl rotation for glucopyranose derivatives. The results of ab initio calculations on D-glucose[1,25−27] and on model compounds[28,29] suggest that solvation and intramolecular hydrogen bonding are very important. Semiempirical calculations[30] and molecular dynamics simulations[27,31−33] on glucose also implicated solvation. The goal of this work is to provide unambiguous experimental evidence about the role of solvent effects and other effects on the rotamer population of the hydroxymethyl group in glucopyranose derivatives and to define more precisely the mechanisms through which the solvent effects operate.

Solvent effects and hydrogen bonding are interrelated and thus are difficult to evaluate separately. Most NMR studies have been performed almost exclusively in aqueous solutions or in polar solvents, such as methanol, DMSO, or acetonitrile.[2,14] Intramolecular hydrogen bonding may have a particularly strong influence on the relative stabilities of the *tg* rotamers for aldohexopyranose derivatives with O4 in an equatorial orientation.[34] Bock and Duus explored hydrogen bonding with ^{1}H NMR spectroscopy in polar solvents and did not find evidence for significant contributions.[2] A study of glucose in DMSO also indicated that hydrogen bonding was only present to a very limited extent.[35] Infrared spectroscopy, optical rotation, and NMR spectroscopy[34,36] have indicated that, for pyran and cyclohexane models of aldohexopyranosides, there was significant intramolecular hydrogen bonding in nonpolar solvents. Theoretical studies have suggested that intramolecular hydrogen bonding of OH6 to O5 is a major factor in the stability of the *gg* and *gt* rotamers, even in water.[29]

A number of experimental techniques have been used to examine the rotamer populations of hexopyranosides. The technique used most commonly is NMR spectroscopy,[2−4,6,7,11,17,23,24] mainly via analysis of coupling constants involving H6R and H6S but also through proton−proton relaxation rates[24b,37] and methods that combine several measurements.[37,38] Information has also been obtained through the statistical analysis of X-ray crystal data[39] and by optical techniques.[5,13,24b,36,40] The rotamer populations determined by these methods are consistent within wide ranges. For glucopyranoside derivatives, the percentage populations for the *gg*, *gt*, and *tg* rotamers are 45−70%, 30−55%, and −25 to 25%, respectively.[2−5,8,10,14,15,19,20,23,24] Similar results are obtained for mannose derivatives.[7,9,11,16,17] For galactopyranose derivatives, the corresponding percentages are 10−25%, 55−78%, and 2−30%.[2,4,6,9−12,15,18,21,23,24]

A major problem with the determination of rotamer populations using *vicinal* H,H coupling constants has been that variable negative populations of the *tg* rotamer are often obtained, which can be as large as −25%.[2,3,8,17,19,24b] To calculate these populations, estimates of the coupling constants for each rotamer must be obtained in some manner and inaccurate values from these estimates are probably the most important cause of this problem. A second factor may be the use of inaccurate values of measured coupling constants, perhaps arising from performing first-order analyses of ^{1}H NMR coupling patterns for which a second-order analysis is more appropriate. The normal solution to the problem of negative populations of the *tg* rotamer is to assume that its population is zero.[2] This procedure is satisfactory for evaluating the relative stabilities of the *gg* and *gt* rotamers, but it automatically obscures any trends in changes of the populations of the *tg* rotamer.

The incorporation of other data such as proton−proton cross relaxation data and/or NOE data is appealing as a way to avoid the above difficulty.[24,37,38] However, these data are considerably less precise than carefully measured coupling constants and are probably also less accurate. *Vicinal* C,H coupling constants can also be useful in this regard,[24] but the smaller amount of data available[41,42] for well-defined geometries has resulted in a less precise definition of substituent effects on magnitudes of these values than for the comparable H,H data. Therefore, we have chosen to use the most accurate data, the H,H coupling constants, and have attempted to minimize the uncertainties implicit in their use by reexamining the geometric and thermodynamic models needed to employ them.

(25) Brown, J. W.; Wladkowski, B. D. *J. Am. Chem. Soc.* **1996**, *118*, 1190−1193.
(26) (a) Polavarapu, P. L.; Ewig, C. S. *J. Comput. Chem.* **1992**, *13*, 1255−1261. (b) Salzner, U.; Schleyer, P. v. R. *J. Org. Chem.* **1994**, *59*, 2138−2155. (c) Barrows, S. E.; Dulles, F. J.; Cramer, C. J.; French, A. D.; Truhlar, D. G. *Carbohydr. Res.* **1995**, *276*, 219−251.
(27) Molteni, C.; Parrinello, M. *J. Am. Chem. Soc.* **1998**, *120*, 2168−2171.
(28) Zheng, Y.-J.; Le Grand, S. M.; Merz, K. M., Jr. *J. Comput. Chem.* **1992**, *13*, 772−791.
(29) Tvaroška, I.; Carver, J. P. *J. Phys. Chem. B* **1997**, *101*, 2992−2999.
(30) (a) Tvaroška, I.; Imberty, A.; Pérez, S. *Biopolymers* **1990**, *30*, 369−379. (b) Tvaroška, I.; Kožár, T. *Theor. Chim. Acta* **1986**, *70*, 99−114. (c) Cramer, C. J.; Truhlar, D. G. *J. Am. Chem. Soc.* **1993**, *115*, 5745−5753.
(31) (a) Brady, J. W. *J. Am. Chem. Soc.* **1986**, *108*, 8153−8160. (b) Brady, J. W. *J. Am. Chem. Soc.* **1989**, *111*, 5155−5165. (c) Ha, S.; Gao, J.; Tidor, B.; Brady, J. W.; Karplus, M. *J. Am. Chem. Soc.* **1991**, *113*, 1553−1557.
(32) (a) Kroon-Batenburg, L. M. J.; Kroon, J. *Biopolymers* **1990**, *29*, 1243−1248. (b) van Eijck, B. P.; Hooft, R. W. W.; Kroon, J. *J. Phys. Chem.* **1993**, *97*, 12093−12099.
(33) (a) Glennon, T. M.; Zheng, Y.-J.; Le Grand, S. M.; Shutzberg, B. A.; Merz, K. M., Jr. *J. Comput. Chem.* **1994**, *15*, 1019−1040. (b) Cheetham, N. W. H.; Lam, K. *Carbohydr. Res.* **1996**, *282*, 13−23.
(34) Beeson, C.; Pham, N.; Shipps, G., Jr.; Dix, T. A. *J. Am. Chem. Soc.* **1993**, *115*, 6803−6812.
(35) Angyal, S. J.; Christofides, J. C. *J. Chem. Soc., Perkin Trans. 2* **1996**, 1485−1491.
(36) (a) Lemieux, R. U.; Martin, J. C. *Carbohydr. Res.* **1970**, *13*, 139−161. (b) Lemieux, R. U.; Brewer, J. T. In *Carbohydrates in Solution*; Gould, R. F., Ed.; American Chemical Society: Washington DC, 1971; pp 121−146.
(37) Poppe, L. *J. Am. Chem. Soc.* **1993**, *115*, 8421−8426.
(38) Džakula, Z.; Westler, W. M.; Markley, J. L. *J. Magn. Reson., Ser. B* **1996**, *111*, 109−126.
(39) (a) Marchessault, R. H.; Perez, S. *Biopolymers* **1979**, *18*, 2369−2374. (b) Kouwijzer, M. L. C. E.; Grootenhuis, P. D. J. *J. Phys. Chem.* **1995**, *99*, 13426−13436.
(40) Liu, H.-W.; Nakanishi, K. *J. Am. Chem. Soc.* **1981**, *103*, 5591−5593.
(41) Tvaroška, I.; Taravel, F. R. *Adv. Carbohydr. Chem. Biochem.* **1995**, *51*, 15−61.
(42) (a) Tvaroška, I.; Gajgos, J. *Carbohydr. Res.* **1995**, *271*, 151−162. (b) Podlasek, C. A.; Wu, J.; Stripe, W. A.; Bondo, P. B.; Serianni, A. S. *J. Am. Chem. Soc.* **1995**, *117*, 8635−8644. (c) Hayes, M. L.; Serianni, A. S.; Barker, R. *Carbohydr. Res.* **1982**, *100*, 87−101.

To minimize the number of variables in this study, we have chosen to examine methyl 2,3,4,6-tetra-*O*-[$^2H_3$]methyl-α-D-glucopyranoside (**2a**) and methyl 2,3,4-tri-*O*-[$^2H_3$]methyl-α-D-glucopyranoside (**6**). These compounds are sufficiently soluble in a wide range of solvents as to allow solvation studies. The effects of solvation on NMR chemical shifts are examined and shown to be influenced by some of the same factors that affect hydroxymethyl rotamer populations.

Experimental Section

General Methods. Most NMR spectra were run at 300 K in high-quality 5-mm NMR tubes on Bruker AMX-600, -500, or -400 instruments at concentrations between 10 and 15 mM. The spectra of **8** and **9** were recorded on a Bruker AC-250 NMR spectrometer at concentrations between 1.5 and 8 mM or, where necessary, at 400 MHz on a Bruker AMX-400. Chemical shifts are given in parts per million (±0.01 ppm) relative to TMS (chloroform-*d* and CS_2) or referenced to a solvent line as an internal standard as follows: cyclohexane-d_{12}, 1.38 ppm (singlet); toluene-d_{12}, 2.05 ppm (quintet); tetrahydrofuran-d_{12}, 1.73 ppm (singlet); dichloromethane-d_2, 5.32 ppm (triplet); acetone-d_{12}, 2.05 ppm (quintet); methanol-d_4, 3.31 ppm (quintet); acetonitrile-d_3, 1.94 ppm (quintet); dimethyl sulfoxide-d_{12}, 2.50 ppm (quintet); water-d_2, 4.63 ppm (singlet). Spectral patterns were analyzed initially by first- or second-order[43] methods followed by iterative simulation with the program LAME8[44] to give coupling constants, for which the largest uncertainty was ±0.05 Hz. The average difference between transitions in experimental and calculated spectra was 0.15 Hz, and largest differences were typically 0.49 Hz. Infrared spectra were recorded on a Nicolet 510P FTIR spectrometer using NaCl solution cells with lead spacers for solutions.

Sodium hydride was purchased from Aldrich as a 60% dispersion in mineral oil, then washed repeatedly with pentane in an argon atmosphere before use. *N*,*N*-Dimethylformamide was dried over $MgSO_4$ for 48 h followed by vacuum distillation and stored over 4-Å molecular sieves. Pyridine was dried by reflux and distillation over calcium hydride. Anhydrous methanol was obtained by reflux and distillation over $Mg(OMe)_2$. Anhydrous THF was obtained by predistillation over P_2O_5 followed by reflux and distillation over sodium/benzophenone. Amberlite IR-120(+) ion-exchange resin was purchased from Aldrich and prepared for use in the H^+ form by gentle stirring for 24 h in 1.0 M HCl, filtration, and rinsing with anhydrous methanol. All solvents used for extraction and recrystallization were distilled before use. Melting points were determined with a Fisher−Johns melting point apparatus and are uncorrected. Specific rotations were measured on a Perkin-Elmer model 141 polarimeter. Mass spectra were run on a Dupont-CEC 21-110 (electron ionization (EI)) double-focusing mass spectrometer with an EI energy of 70.0 eV. Thin-layer chromatography was performed on 0.20-mm-thick Merck silica gel 60F-254 aluminum plates. Components were visualized by spraying with a 2% ceric sulfate solution in 1 M H_2SO_4 followed by heating on a hot plate until discoloration occurred. Dry column flash chromatography was performed on TLC grade silica gel using a gradient elution from hexane to ethyl acetate.

Methyl 2,3,4,6-Tetra-*O*-[$^2H_3$]methyl-α-D-glucopyranoside (2a). Methyl α-D-glucopyranoside (**1**) (1.51 g, 7.8 mmol) was methylated using the technique of Brimacombe et al.,[45] but using [$^2H_3$]methyl iodide (99%). The product was distilled using a bulb to bulb distillation apparatus to give 1.48 g (72%) of **2a** as a clear oil: bp 98 °C/1.3 kPa, lit.[46] bp 145 °C/1.8 kPa; $[\alpha]^{22}_D$ +141° (*c* 0.68, MeOH), lit.[46,47] $[\alpha]^{20}_D$ +140° (*c* 1.0, H_2O); MS *m*/*z* 231 (0.78%, $M^+ - OCH_3$).

Methyl α-D-[4-^{13}C]Glucopyranoside (3). D-[4-^{13}C]Glucose (99%)-(248.9 mg, 1.37 mmol) was converted to methyl α-D-[4-^{13}C]glucopyranoside (70 mg, 26%) by the method of Bollenback:[48] mp 165−166 °C, lit.[48] 166−167 °C.

Methyl 2,3,4,6-Tetra-*O*-[$^2H_3$]methyl-α-D-[4-^{13}C]glucopyranoside (2b). Compound **3** was methylated as for compound **1** above to give a clear oil (30.2 mg, 35%): $[\alpha]^{22}_D$ +140° (*c* 0.22, MeOH), lit.[46,47] $[\alpha]^{20}_D$ +140° (*c* 1.0, H_2O); MS *m*/*z* 232 (1.0%, $M^+ - OCH_3$).

Methyl 6-*O*-(*tert*-Butyldimethylsilyl)-α-D-glucopyranoside (4). Compound **1** (3.88 g, 20 mmol) and *tert*-butyldimethylsilyl chloride (3.32, 22 mmol) were dissolved in pyridine (40 mL) and stirred overnight at room temperature. Water (25 mL) was added, and the mixture was extracted with ether (5 × 40 mL). The combined extracts were dried ($MgSO_4$) and concentrated to a solid residue that was recrystallized from hexanes−ether to give **4** (3.08 g, 50%) as a colorless solid: mp 155−156 °C, lit.[49] 155−157 °C; ^{1}H NMR spectrum identical to lit.;[49] ^{13}C NMR ($CDCl_3$, 62.9 MHz, δ) 99.2 (C1), 74.5 (C3), 72.1 (C5), 71.7 (C2), 71.0 (C4), 63.8 (C6), 55.1 (OMe), 25.9 (−C(*C*H$_3$)$_3$), 18.3 (−*C*(CH$_3$)$_3$).

Methyl 2,3,4-Tri-*O*-[$^2H_3$]methyl-6-*O*-(*tert*-butyldimethylsilyl)-α-D-glucopyranoside (5). Compound **4** was methylated by the method used to prepare **2a** and **2b**. The title compound (**5**) was purified by dry-column flash chromatography to give a clear oil (1.07 g, 30%): ^{1}H NMR spectrum identical to lit.;[49] ^{13}C NMR ($CDCl_3$, 62.9 MHz, δ) 97.3 (C1), 83.6 (C3), 81.8 (C2), 79.1 (C4), 71.4 (C5), 62.1 (C6), 54.9 (O*C*H$_3$), 25.9 (−C(*C*H$_3$)$_3$), 18.3 (−*C*(CH$_3$)$_3$).

Methyl 2,3,4-Tri-*O*-[$^2H_3$]methyl-α-D-glucopyranoside (6). Compound **5** (1.07 g, 3 mmol) was desilylated by the method of Franke and Guthrie[49] to give **6** after chromatography as a colorless oil (226.9 mg, 30%): $[\alpha]^{22}_D$ +150° (*c* 0.1, $CHCl_3$); lit.[47,50] $[\alpha]^{20}_D$ +150° (*c* 0.1, $CHCl_3$); ^{13}C NMR ($CDCl_3$, 62.9 MHz, δ) 97.6 (C1), 83.3 (C3), 81.8 (C2), 79.6 (C4), 70.5 (C5), 62.0 (C6), 55.2 (O*C*H$_3$); MS *m*/*z* 214 (1.3%, $M^+ - OCH_3$).

Methyl 2,3,4,6-Tetra-*O*-acetyl-α-D-glucopyranoside (8) and Methyl 2,3,4,6-Tetra-*O*-benzoyl-α-D-glucopyranoside (9). Compound **1** was acetylated and benzoylated using standard techniques to give compound **8** (mp 100−102 °C, lit.[51] mp 100−101 °C) and compound **9** (mp 106−108 °C, lit.[52] mp 105 °C, lit.[53] mp 107−108 °C).

Results

Methyl 2,3,4,6-tetra-*O*-[$^2H_3$]methyl-α-D-glucopyranoside (**2a**), methyl 2,3,4,6-tetra-*O*-[$^2H_3$]methyl-α-D-4-[^{13}C]glucopyranoside (**2b**), and methyl 2,3,4-tri-*O*-[$^2H_3$]methyl-α-D-glucopyranoside (**6**) were synthesized from methyl α-D-glucopyranoside (**1**) or D-[4-^{13}C]glucose by methods identical to or similar to those used for preparation of their nonlabeled analogues.[45,46,49]

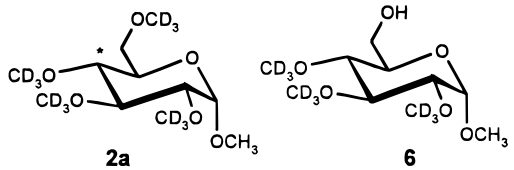

2a **6**

2b * = ^{13}C

The ^{1}H NMR spectra of **2a** and **6** were recorded in a range of solvents mostly at 600 and 500 MHz, respectively. The seven spin patterns due to H1, H2, H3, H4, H5, H6R, and H6S in the spectra of **2a** and the eight spin patterns due to the above protons

(43) Garbisch, E. W., Jr. *J. Chem. Educ.* **1968**, *45*, 311−321; **1968**, *45*, 402−416; **1968**, *45*, 480−493.
(44) Haigh, C. W. *Ann. Rep. NMR Spectrosc.* **1971**, *4*, 311−362.
(45) Brimacombe, J. S.; Jones, B. D.; Stacey, M.; Willard, J. J. *Carbohydr. Res.* **1966**, *2*, 167−169.
(46) Hirst, E. L.; Percival, E. In *Methods in Carbohydrate Chemistry*; Whistler, R. L., Wolfrom, M. L., Eds.; Academic Press: New York, 1963; Vol. II, pp 145−150.
(47) The literature optical rotations were adjusted for changes in molecular weight due to isotopic substitution.
(48) Bollenback, G. N. In *Methods in Carbohydrate Chemistry*; Whistler, R. L., Wolfrom, M. L., Eds.; Academic Press: New York, 1963; Vol. II, pp 326−327.
(49) Franke, F.; Guthrie, R. D. *Aust. J. Chem.* **1977**, *30*, 639−647.
(50) Klemer, A.; Bieber, M.; Wilburs, H. *Liebigs Ann. Chem.* **1983**, 1416−1421.
(51) Hudson, C. S.; Dale, J. K. *J. Am. Chem. Soc.* **1915**, *37*, 1264−1270.
(52) Helferich, B.; Becker, J. *Liebigs Ann. Chem.* **1924**, *440*, 1−18.
(53) Pelyvás, I. F.; Lindhorst, T. K.; Streicher, H.; Thiem, J. *Synthesis* **1991**, 1015−1020.

Table 1. NMR[a] Data for H6R and H6S and Rotamer Populations of Methyl 2,3,4,6-Tetra-*O*-[$^2H_3$]methyl-α-D-glucopyranoside (**2a**)

solvent	dielectric constant (ϵ)	chemical shifts (ppm)		coupling constants (Hz)		rotamer populations[b,c] (%)		
		H6R	H6S	$^3J_{5,6R}$	$^3J_{5,6S}$	*gg*	*gt*	*tg*
C_6D_{12}[d]	2.0	3.52	3.38	4.49	1.64	67 (63)	39 (37)	−6
$C_6D_5CD_3$[d]	2.4	3.55	3.47	4.79	1.48	65 (60)	43 (40)	−8
CS_2	2.6	3.43	3.34	4.90	1.70	62 (59)	43 (41)	−5
$CDCl_3$	4.8	3.59	3.57	4.02	2.42	67	30	3
THF-d_8	7.6	3.51	3.45	4.94	1.82	61 (59)	43 (41)	−4
CD_2Cl_2	8.9	3.53	3.51	4.52	2.21	62	37	1
$(CD_3)_2CO$	20.7	3.51	3.49	4.80	2.08	60 (60)	41 (40)	−1
CD_3OD	32.7	3.57	3.54	4.66	1.96	63 (62)	39 (38)	−2
CD_3CN	37.5	3.49	3.48	4.75	2.48	57	39	4
D_2O[d]	78	3.51	3.53	4.64	2.43	59	37	4

[a] Spectra recorded at 600 MHz unless otherwise noted. [b] Determined using eqs 1−3, with ^3J values from Table 4. [c] Values in parentheses calculated assuming that the population of the *tg* rotamer was 0%. [d] Recorded at 400 MHz.

Table 2. NMR[a] Data for H6R and H6S and Rotamer Populations of Methyl 2,3,4-Tri-*O*-[$^2H_3$]methyl-α-D-glucopyranoside (**6**)

solvent	dielectric constant (ϵ)	chemical shifts (ppm)		coupling constants (Hz)		rotamer populations[b,c] (%)		
		H6R	H6S	$^3J_{5,6R}$	$^3J_{5,6S}$	*gg*	*gt*	*tg*
C_6D_{12}[d]	2.0	3.58	3.65	3.25	2.86	73	18	9
CS_2[d]	2.6	3.81	3.91	4.00	2.78	68	28	4
$CDCl_3$	4.8	3.75	3.84	4.14	3.09	60	28	12
$(CD_3)_2CO$	20.7	3.62	3.71	4.61	2.06	63	37	0
CD_3OD	32.7	3.66	3.72	4.66	2.06	62	38	0
CD_3CN	37.5	3.57	3.67	4.85	2.16	59	40	1
DMSO-d_6	46.7	3.47	3.57	5.48	1.13	58 (52)	53 (48)	−11
D_2O	80.2	3.55	3.64	4.84	1.90	61 (60)	41 (40)	−2

[a] Spectra recorded at 500 MHz unless noted otherwise. [b] Determined using eqs 1−3, with ^3J values from Table 4. [c] Values in parentheses calculated assuming that the population of the *tg* rotamer was 0%. [d] Recorded at 400 MHz.

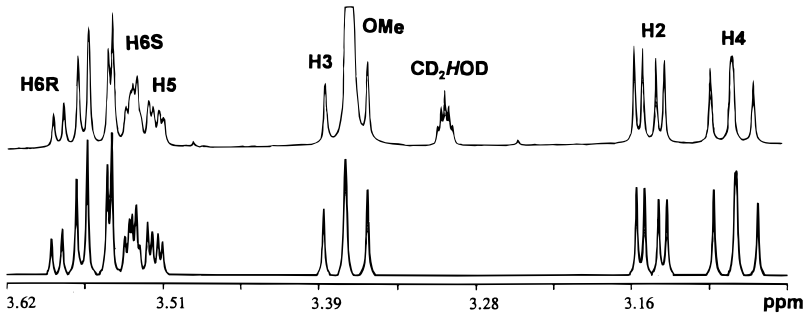

Figure 2. Part of the experimental 600-MHz ^1H spectrum of methyl 2,3,4,6-tetra-*O*-[$^2H_3$]methyl-α-D-glucopyranoside in methanol-d_4 and the simulated spectrum: top, experimental spectrum; bottom, simulation using LAME8.[44]

and to OH6 of **6** were iteratively simulated as outlined in the Experimental Section. The results for the H6R−H6S parts of the simulations in the various solvents are listed in Table 1 for **2a** and Table 2 for **6**.[54,55] An example of the fit obtained is presented in Figure 2. The spectra from CS_2 and cyclohexane-d_{12} solutions of **6** could not be analyzed in the region containing the H6R/H6S/H5 subspectra until the broadening caused by coupling to the hydroxyl proton was removed by exchange. This was performed by repeatedly shaking a sample of **6** in water-d_2 followed by azeotropic removal of the water-d_2 with toluene.

Unambiguous identification of the H6R and H6S signals is required to employ these NMR results for analysis of rotamer populations. Stereospecifically deuterated compounds[56] or $^3J_{CH}$ coupling constants from ^{13}C-enriched compounds[41,42] have both been used for this purpose. For **2a**, the H6R and H6S signals were assigned by examination of the $^{13}C-C-C-H$ coupling constants from the NMR spectra of methyl 2,3,4,6-tetra-*O*-[$^2H_3$]-methyl-α-D-[4-^{13}C]glucopyranoside (**2b**). The NMR spectra were analyzed as for **2a** above (see Figure 3). The data for the prochiral H6's are found in Table 3.

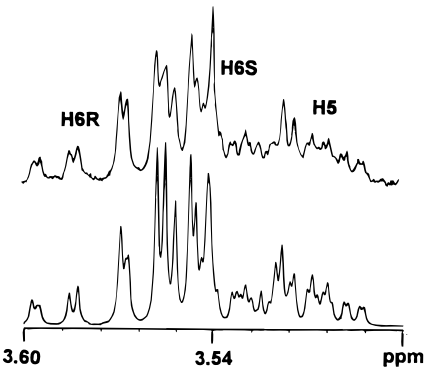

Figure 3. Part of the experimental 400-MHz ^1H spectrum of methyl 2,3,4,6-tetra-*O*-[$^2H_3$]methyl-α-D-[4-^{13}C]glucopyranoside in methanol-d_4 containing the signals of H5, H6S, and H6R and its simulated spectrum: top, experimental spectrum; bottom, simulation using LAME8.[44]

The correct assignment was made by determining which assignment best fit both the experimental $^3J_{C4,H6}$ and $^3J_{5,6}$'s. For

(54) Tables containing the complete simulation results for the seven spin patterns are included in the Supporting Information.

(55) H6R and H6S refer to the *pro-R* and *pro-S* protons, respectively.

(56) (a) Ohrui, H.; Horiki, H.; Kishi, H.; Meguro, H. *Agric. Biol. Chem.* **1983**, *47*, 1101−1106. (b) Ohrui, H.; Nishida, Y.; Meguro, H. *Agric. Biol. Chem.* **1984**, *48*, 1049−1053.

Table 3. NMR Data from the Analysis of the Spectra of Methyl 2,3,4,6-Tetra-*O*-[$^2H_3$]methyl-α-D-4-[^{13}C]glucopyranoside (**2b**)

solvent	dielectric constant (ϵ)	chemical shifts (ppm) H-6R	H-6S	coupling constants[a] (Hz) $^3J_{5,6R}$	$^3J_{5,6S}$	$^3J_{C4,H6R}$	$^3J_{C4,H6S}$
C_6D_{12}	2.0	3.52	3.38	4.37	1.56	0.01	3.20
$C_6D_5CD_3$	2.4	3.56	3.48	4.59	1.72	0.36	3.09
CD_3OD	32.7	3.57	3.54	4.62	2.03	0.76	3.16

[a] As determined from LAME8[44] iterative analysis.

example, using the data for **2a** in methanol-d_4 (Table 1), assigning H6R as the high-frequency proton and H6S as the low-frequency proton gave a *gg*:*gt*:*tg* rotamer ratio of 61:39:0, calculated as described below. For the reverse assignment, the rotamer ratio was 72:0:28, respectively. Using the $^3J_{CH}$ values from Tvaroska[41,42] ($^3J_{C4,H6R}(gg/gt/tg)$ = 0.73 Hz/0.73 Hz/ 7.92 Hz; $^3J_{C4,H6S}(gg/gt/tg)$ = 7.90 Hz/1.89 Hz/1.26 Hz), the values for $^3J_{C4,H6R}$ and $^3J_{C4,H6S}$ were calculated for each assignment. The first assignment gives calculated $^3J_{C4,H6R}$ and $^3J_{C4,H6S}$ of 0.73 and 5.56 Hz, respectively, and the second assignment, 2.75 and 6.04 Hz, respectively. Only $^3J_{C4,H6R}$ is calculated to have markedly different values for the two assignments, and the first assignment fits the experimental coupling constant exactly (see Table 3).

In all solvents except water-d_2, the signal due to H6R appears at a higher frequency than that of H6S. However, simulation of the patterns observed in water-d_2 of compound **2b** with LAME8[44] using both assignments allowed the unambiguous assignment of the higher frequency signal to H6S in this solvent.

The assignment of the prochiral protons on C6 of **6** was based on two facts. First, in all glucopyranose derivatives except those where O4 and O6 bear small substituents, the signal of H6S appears at a higher frequency than of H6R.[2] Second, the assignment should be such that in the most nonpolar solvent (cyclohexane-d_{12}), the *tg* population should be at a maximum due to intramolecular hydrogen bonding (see below). In the spectrum of the cyclohexane-d_{12} solution of **6**, the coupling constants are nearly identical and thus the assignment of the protons does not affect the calculation of the rotamer populations significantly; assigning the low-frequency signal as H6S results in a *gg*:*gt*:*tg* rotamer ratio of 73:18:9, while the opposite assignment gives 75:12:13. The assignments in more polar solvents should result in a decreased *tg* population. The result of the assignments based on these facts is that in all solvents the signal of H6S appears at a higher frequency than that of H6R for **6** in agreement with that observed for most glucopyranoside derivatives.

Rotamer Populations. Once the assignments of H6R and H6S have been made reliably, rotamer populations can be obtained from the two $^3J_{5,6}$ values if the coupling constants for each rotamer are known. Bock and Duus[2] compared the various strategies used for obtaining these values, including the use of different types of model compounds with fixed geometries,[2,3,5757] the use of values calculated from the Haasnoot−Altona modification of the Karplus equation,[5858] and the use of vibrationally averaged calculated values. They were unable to decide which method gave the best results but concluded that the similarity of the results when the population of the *tg* rotamer was set to zero allowed the use of the most convenient calculated values.

Two aspects of this approach have been further investigated here. First, the geometries of the minima have been improved.

Table 4. Torsional Angles and Limiting Coupling Constants for Methyl 2,3,4,6-Tetra-*O*-[$^2H_3$]methyl-α-D-glucopyranoside (**2a**) and Methyl 2,3,4-Tri-*O*-[$^2H_3$]methyl-α-D-glucopyranoside (**6**)

compd	rotamer	torsional angles (deg)[a] H5−C5−C6−H6R	H5−C5−C6−H6S	O5−C5−C6−O6	limiting coupling constants (Hz) $^3J_{5,6R}$	$^3J_{5,6S}$
2a	*gg*	51.9	−66.1	−69.9	1.61	2.25
	gt	−169.4	71.7	71.7	9.47	1.94
	tg	−65.8	175.9	173.2	4.11	10.61
6	*gg*	51.4	−66.6	−70.6	1.61	2.16
	gt	−168.5	72.5	72.6	9.47	1.94
	tg	−66.7	175.0	171.3	3.97	10.59

[a] Angles calculated using MM3(94) with modified OCCO torsional parameters

Bock and Duus[2] used perfectly staggered angles for the rotameric minima (180° and ±60°); here, these angles have been taken from minima calculated for **2a** using MM3(94) with improved O−C−C−O torsional parameters.[59] The geometry of **2a** employed in these calculations had the glycosidic OMe in the exo anomeric position, the methyl groups on O-2 to O-4 gauche to the hydrogen atoms on the attached carbons and oriented toward O-1, and the methyl on O-6 anti to C-5. The stabilities of conformers having all other staggered orientations of the methoxy groups were evaluated, but none were found that contained more than 13% of the most populated conformer. The torsional angles calculated for the rotameric minima and the coupling constants obtained from them using the Haasnoot−Altona equation[58] are listed in Table 4.

Second, we have also examined the effects of a more sophisticated approach to vibrational averaging on the magnitudes of the coupling constants. Because the Karplus equation is not symmetrical about the torsional angles present in the rotameric minima, it might be expected that vibrational averaging would result in different values for rotamer coupling constants than obtained by using the minimum energy geometries. For instance, vibrational averaging about a 180° angle can only decrease the calculated coupling constant which is at a maximum at 180°. Bock and Duus[2] evaluated this factor by calculating three different potential energy surfaces with 3-fold potentials using 1° grid searches. Each surface was totally symmetrical with barriers at the eclipsed conformations of 1, 2, or 3 kcal/mol. The resulting values gave populations that were significantly worse (i.e., more negative *tg* rotamer populations) than the values calculated directly from the rotameric minima.[2]

We perceive two problems with this approach. First, the parameters in the Haasnoot−Altona curve were derived[58] without considering the effects of vibrational averaging; therefore, the parameters already incorporate these effects to some degree. The list of model compounds used in the derivation of these parameters was not provided,[58] but it is stated that all were cyclic. The greater barriers in cyclic compounds will cause vibrational averaging to be less important than for the exocyclic system considered here. Therefore, vibrational averaging should in theory cause the magnitudes of $^3J_{5,6}$ values for individual hydroxymethyl rotamers calculated from the Haasnoot−Altona equation to be somewhat different than the actual values of coupling constants for all rotameric energy wells. Second and more importantly, all three saddle points on the C5−C6 rotational potential energy surface are different and neither the minima nor the saddle points have ideal torsional angles.

(57) Manor, P. C.; Saenger, W.; Davies, D. B.; Jankowski, K.; Rabczenko, A. *Biochim. Biophys. Acta* **1974**, *340*, 472−483.

(58) Haasnoot, C. A. G.; DeLeeuw, F. A. A. M.; Altona, C. *Tetrahedron* **1980**, *36*, 2783−2792.

(59) Rockwell, G. D.; Grindley, T. B. *Aust. J. Chem.* **1996**, *49*, 379−390.

Table 5. Saddle Point Geometries and Energies for Methyl 2,3,4,6-Tetra-*O*-methyl-α-D-glucopyranoside[a]

conformer	torsional angles (deg) O5−C5−C6−O6	torsional angles (deg) C4−C5−C6−O6	strain energy[b] (kJ mol^{-1})	frequency[c] (cm^{-1})
syn-O5[d]	−0.4	120.1	35.5	−130.5
syn-C4[d]	−128.8	−8.2	18.8	−104.3
syn-H5[d]	124.1	−116.5	12.7	−76.0

[a] Calculated using MM3(94) with modified OCCO torsional parameters.[59] [b] Relative to the conformer calculated to be the global minimum, the *gt* conformer. [c] The imaginary frequency for the vibration which corresponds to motion over the saddle point, listed by MM3 as a negative number. [d] Named according to the atom syn to O-6 in the saddle point.

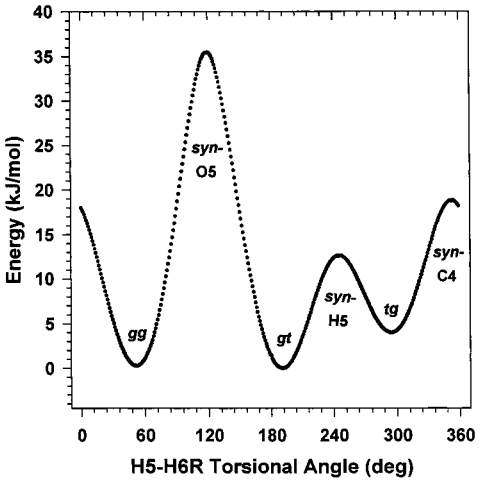

Figure 4. Plot of relative enthalpy from MM3(94)[59] versus H5−C5−C6−H6R torsional angle for methyl 2,3,4,6-tetra-*O*-methyl-α-D-glucopyranoside (**2a**).

These factors have been evaluated by locating the saddle points by dihedral angle driving using MM3(94) followed by full-matrix Newton−Raphson minimization of the saddle point geometries to give conformations with one imaginary infrared frequency. Then, the dihedral angle driving from the saddle points to the minima gave a 1° energy grid that was used to generate Boltzman distributions in each energy well. This approach to defining a potential energy surface avoids the hysteresis effects commonly observed just beyond the saddle points, when dihedral angle driving is used to proceed from one minima to another. The Boltzman distributions were then employed to determine average coupling constants for each well from the calculated[58] coupling constants at each point on the grid. The geometries and energies of the saddle points are listed in Table 5. Saddle points are named according to the atom that is eclipsed with O6. Figure 4 shows a representation of the C5−C6 rotational potential energy surface calculated in this way.

This calculation suggests that the barrier ($\Delta H^{\ddagger}$) to interconversion of the *gg* and *gt* rotamers via the *tg* rotamer and the *syn*-C4 saddle point would be 18.8 kJ-mol^{-1}. The barrier to this rotation for D-glucose and methyl β-D-glucopyranoside was calculated from results in a paper[60] on the ultrasonic relaxation of these compounds to be 19.2 kJ-mol^{-1} if it is assumed that the *gg* and *gt* rotamers are equally populated, in excellent agreement with the calculation.

Although vibrational averaging should influence the rotameric coupling constants to some extent, the results shown in Table 6 indicate that its incorporation has very small effects on the calculated rotameric populations. The major effect observed, a decrease in the population of the *tg* rotamer to negative values, must be incorrect. Therefore, we decided to use the coupling constants calculated directly from the geometries of the rotameric minima for both compounds **2a** and **6**.

Table 6. Comparison of Coupling Constants and Populations of **2a** Obtained with and without Vibrational Averaging

		gg	*gt*	*tg*
coupling constants calcd without vibrational averaging (Hz)	$^3J_{H5,H6R}$	1.61	9.47	4.11
	$^3J_{H5,H6S}$	2.25	1.94	10.61
calculated populations	in C_6D_{12}	67	39	−6
	in $CDCl_3$	67	30	3
	in CD_3OD	63	39	−2
	in D_2O	59	37	4
coupling constants calcd with vibrational averaging (Hz)	$^3J_{H5,H6R}$	1.92	9.10	4.13
	$^3J_{H5,H6S}$	2.40	2.15	10.09
calculated populations	in C_6D_{12}	70	38	−9
	in $CDCl_3$	70	29	1
	in CD_3OD	65	40	−4
	in D_2O	61	37	2

Table 7. NMR Data[a] for the OH Proton of Compound **6**

solvent	chemical shift (ppm)	coupling constant (Hz) $^3J_{OH,H6R}$	coupling constant (Hz) $^3J_{OH,H6S}$	rotamer populations[b] (%) I[c]	rotamer populations[b] (%) II[c]	rotamer populations[b] (%) III[c]
$CDCl_3$	1.85	7.71	4.77	17	56	27
$(CD_3)_2CO$	3.55	7.10	5.44	16	50	34
CD_3CN	2.68	6.72	5.51	19	46	35
$(CD_3)_2SO$	4.67	6.29	5.60	23	42	35

[a] Determined from 500-MHz spectra. [b] Determined using equations from Fraser et al.[62] [c] See Figure 5.

Once limiting values of the coupling constants have been obtained, the rotameric mole fractions can be evaluated from eqs 1−3:

$$^3J_{H5,H6R} = {}^3J_{R,gg}\,f_{gg} + {}^3J_{R,gt}\,f_{gt} + {}^3J_{R,tg}\,f_{tg} \quad (1)$$

$$^3J_{H5,H6S} = {}^3J_{S,gg}\,f_{gg} + {}^3J_{S,gt}\,f_{gt} + {}^3J_{S,tg}\,f_{tg} \quad (2)$$

$$1 = f_{gg} + f_{gt} + f_{tg} \quad (3)$$

where f_{gg}, f_{gt}, and f_{tg} are the mole fractions of the three rotamers and the ^3J values are the limiting values of the coupling constants in the three different conformations.

NMR Spectroscopy of the Hydroxyl Proton of Compound 6. The magnitudes of the coupling constants of the OH proton to the prochiral protons of C6 (see Table 7) can reveal information about the orientations of the proton which can, in turn, be correlated with hydrogen bonding. Karplus-type equations have been developed to relate the magnitudes of hydroxyl vicinal coupling constants (H−O−C−H) to the corresponding torsional angles.[61,62] There are three possible staggered rotamers (see Figure 5) about the C6−O6 bond. The limiting values of the coupling constants (J_{gauche} = 2.05 Hz, J_{anti} = 12.1 Hz), calculated with the Karplus relation of Fraser et al.[62] assuming perfectly staggered geometries, were employed to determine hydroxyl rotamer populations using eqs 1−3.

Infrared Spectroscopy of Compound 6. The importance of hydrogen bonding for **6** was also examined by infrared spectrometry. The infrared spectrum was recorded in anhydrous hexane over a range of concentrations from 5 to 20 mM. No

(60) Behrends, R.; Cowman, M. K.; Eggers, F.; Eyring, E. M.; Kaatze, U.; Majewski, J.; Petrucci, S.; Richmann, K. H.; Riech, M. *J. Am. Chem. Soc.* **1997**, *119*, 2182−2186.

(61) Rader, C. P. *J. Am. Chem. Soc.* **1969**, *91*, 3248−3256.

(62) Fraser, R. R.; Kaufman, M.; Morand, P.; Govil, G. *Can. J. Chem.* **1969**, *47*, 403−409.

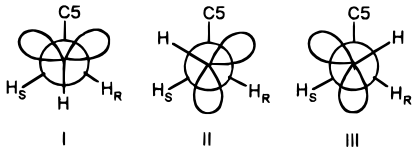

Figure 5. Hydroxyl rotamers about the C6−O6 bond of methyl 2,3,4-tri-*O*-methyl-α-D-glucopyranoside (**6**).

changes in the spectrum were noted over this concentration range, and therefore, it was concluded that intermolecular hydrogen bonding was insignificant. The spectrum (Figure 6) shows a sharp peak and very broad peak. The narrow peak at 3613 cm^{-1} was assigned as the non-hydrogen-bonded signal. The very broad peak was assigned to the OH stretches of different hydrogen bonds. The extinction coefficient of the various O−H stretching peaks could not be determined directly, but estimates of the extinction coefficient for the non-hydrogen bonded peak from the literature[34,36] indicated that 70−96% of the OH6's were hydrogen bonded. The assumption that all of the hydrogen bonding is intramolecular in the *tg* rotamer is not consistent with the results from the analysis of hydroxyl group rotamers from NMR spectroscopy (vide infra). However, this amount of intramolecular hydrogen bonding is reasonable if hydrogen bonding also takes place in rotamers other than the *tg* rotamer.

The infrared spectrum of **6** was also run in acetonitrile, and intramolecular hydrogen bonding was also noted there. This is not surprising given that, even in DMSO, there is evidence that intramolecular hydrogen bonds are present for monosaccharide solutions to a very limited extent.[35] Acetonitrile is not an especially good hydrogen bond acceptor,[63] and the NMR results in this solvent (see Table 2) indicate that the *tg* rotamer is not significantly populated. Therefore, the hydrogen-bonded O−H stretch in acetonitrile must be due to intramolecular hydrogen bonding in the other rotamers.

Reanalysis of Literature Data. The rotamer populations for a series of α-D-glucopyranose derivatives with different substitution at C-4 mostly obtained by Bock and Duus[2] from the $^3J_{H5,H6}$ values measured in water were redetermined using the limiting coupling constants derived for **2a** and **6** above and are listed in Table 8.

Discussion

The accuracy of the analysis of the rotameric populations depends on the values of the limiting coupling constants assigned to each rotamer as well as the accuracy of the experimental coupling constants (see data for α-D-glucopyranose in Table 8). Previous analyses have yielded substantial (<25%) negative populations for the *tg* rotamer of α-D-glucopyranose derivatives.[2−4,8,9,17] These populations must arise either from incorrect values of the limiting coupling constants or inaccuracies in the experimental measurements. The limiting values obtained here using nonstaggered geometries as calculated by MM3 almost eliminate this problem and hence validate the use of these geometries. Surprisingly, incorporation of vibrational averaging does not improve the results.

The nonstaggered geometries obtained by calculation can be compared with geometries from the solid state. The O5−C5−C6−O6 torsional angles calculated here were −70° and −71° for the *gg* rotamer and +72° and +73° for the *gt* rotamer in **2a** and **6**, respectively. Average angles from 101 structures with *gluco* configurations and hydroxymethyl or acyloxymethyl groups were −66.5° for the *gg* rotamer and +65.0° for the *tg* rotamer.[39] However, the steric effects of substituents in the 101 structures on O-6 may alter the inherent preferences toward values that are closer to being perfectly staggered. The O5−C5−C6−O6 angles in the *gt* rotamers in crystals of methyl α-D-glucopyranoside[64] and α-D-glucopyranose[65] were 73.9° and 70.2°, respectively, as determined by neutron diffraction. In α-D-glucopyranose hydrate,[66] the *gg* rotamer had an angle of −67.9°. These values are very similar to the values calculated here and thus also support the use of these calculated values to determine rotameric coupling constants.

Some negative populations values remain (Tables 1 and 2), indicating that there is still a need for improvement either in the geometries or in the calculation of the coupling constants from the geometries. The geometries are probably solvent dependent to some extent and may be slightly different than that calculated by MM3. The calculated coupling constants do not incorporate the effect of changes in bond angles which have been shown[67] to affect their magnitudes to a very small extent at the sizes of bond angles observed at C-6 in the solid state.[39]

Solvent Effects on the Rotameric Equilibria. Surprisingly, the rotamer populations for **2a** in 10 different solvents are essentially independent of the nature of the solvent. There appears to be a slight increase in the population of the *tg* rotamer at the expense of the *gg* rotamer with the population of the *gt* rotamer unchanged, but this observation is at the limit of uncertainty of the method.

This observation is in sharp contrast to those for the two anomers of methyl 2,3,4-tri-*O*-methyl-D-galactopyranoside 6-dimethyl phosphate, where the *gt* rotamer population increased markedly at the expense of the *tg* population as the solvent became more polar.[6] This change was explained as the result of decreasing 1,3-electrostatic repulsions in the *gt* rotamer in polar solvents[6] which stabilize it by 1.0−2.5 kJ with respect to the *tg* rotamer but may be due to the smaller dipole moment of the *tg* rotamer. The *gg* population was unaffected by changes in solvent;[6] therefore, the effect of solvent on its stability must be intermediate between the effects on those of the other two rotamers.

The small size of the observed solvent effect on rotamer populations of compound **2a** can be explained as follows. In nonpolar solvents, the *tg* rotamer is disfavored with respect to the other two rotamers by inherent factors. It has the largest dipole moment (2.72 D calculated by MM3(94) versus 1.35 and 1.90 D for the *gg* and *gt* rotamers, respectively), and its population should be affected by solvent polarity as observed for the more polar rotamer of methyl 2,3,4-tri-*O*-methyl-D-galactopyranoside 6-dimethyl phosphate.[6] However, the population of the *tg* rotamer is below the level of detection in nonpolar solvents. Therefore, the small observed increase with increased solvent polarity (Table 1) is probably real but is difficult to quantify due to the low populations and the uncertainties involved.

For compound **6**, the data in Table 2 reveals that there are significant differences in rotamer populations when going from a nonpolar to a polar solvent (see Figure 7). For instance, when the solvent was changed from cyclohexane-d_{12} to water-d_2, the

(63) Kamlet, M. J.; Abboud, J.-L. M.; Abraham, M. H.; Taft, R. W. *J. Org. Chem.* **1983**, *48*, 2877−2887.

(64) Jeffrey, G. A.; McMullen, R. K.; Takagi, S. *Acta Crystallogr., Sect. B* **1977**, *B33*, 728−737.

(65) Brown, G. M.; Levy, H. A. *Acta Crystallogr., Sect. B* **1979**, *B35*, 656−659.

(66) Hough, E.; Neidle, S.; Rogers, D.; Troughton, P. G. H. *Acta Crystallogr., Sect. B* **1973**, *B29*, 365−367.

(67) (a) Barfield, M.; Smith, W. B. *J. Am. Chem. Soc.* **1992**, *114*, 1574−1581. (b) Barfield, M.; Smith, W. B. *Magn. Reson. Chem.* **1993**, *31*, 696−697. (c) Imai, K.; Osawa, E. *Magn. Reson. Chem.* **1990**, *28*, 668−674.

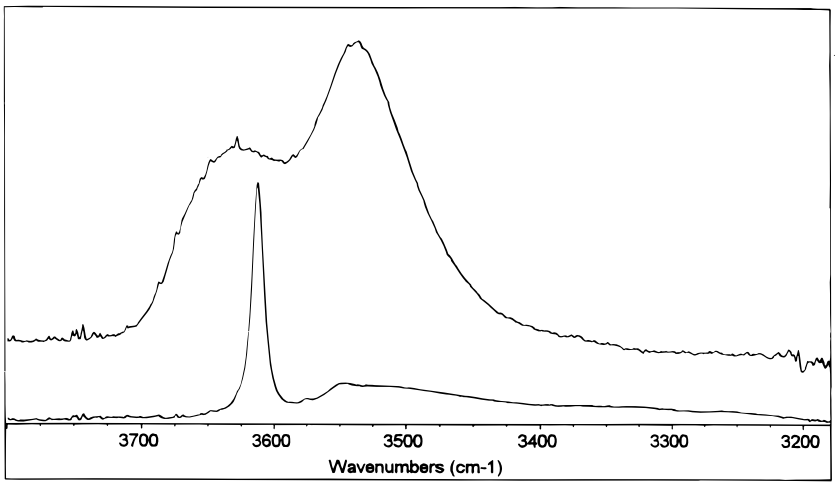

Figure 6. Part of the infrared spectra of methyl 2,3,4-tri-*O*-methyl-α-D-glucopyranoside (**6**) containing OH stretching vibrations in acetonitrile (top) and hexane (bottom). The free OH stretch in acetonitrile is masked by residual water.

Table 8. Observed Coupling Constants and Calculated Rotamer Populations for α-D-Glucopyranose Derivatives in Water-d_2

compd	$^3J_{H5,H6R}$ (Hz)	$^3J_{H5,H6S}$ (Hz)	ref	population (%)[a] *gg*	*gt*	*tg*	population (%)[b] *gg*	*gt*	*tg*
α-D-glucopyranose	5.8	2.8	74	52 (51)	50 (49)	−2	42	50	8
	5.8	1.0	4	65 (52)	60 (48)	−25	55 (49)	57 (51)	−12
	5.8	1.9	3	58 (51)	56 (49)	−14	48 (47)	54 (53)	−2
	5.34	2.21	here	60 (55)	49 (45)	−9	51	47	2
methyl α-D-glucopyranoside (**1**)	5.49[c]	2.39[c]	2	57 (53)	50 (47)	−7	48	48	4
6-*O*-methyl-α-D-glucopyranose[d]	5.73	2.37	2	55 (51)	52 (49)	−7	45	52	3
methyl 2,3,4,6-tetra-*O*-methyl-α-D-glucopyranoside (**2a**)	4.64	2.43	here	66 (62)	40 (38)	−7	59	37	4
methyl 2,3,4-tri-*O*-methyl-α-D-glucopyranoside (**6**)	4.84	1.90	here	68 (60)	45 (40)	−13	61 (60)	41 (40)	−2
methyl 4-deoxy-α-D-glucopyranoside	6.20	3.03	2	45	54	1	33	55	12
methyl 4-amino-4-deoxy-α-D-glucopyranoside	5.40	2.46	2	58 (54)	49 (46)	−6	48	47	5
methyl 4-ammonio-4-deoxy-α-D-glucopyranoside	4.64	3.7	2	56	34	10	48	33	19
methyl 4-deoxy-4-thio-α-D-glucopyranoside	5.0	2.0	2	65 (58)	47 (42)	−12	57	43	0

[a] Calculated using eqs 1−3 and the limiting values used by Bock and Duus.[2] [b] Calculated using eqs 1−3 and the limiting values calculated here (see Table 4) using the values for **2a** for compounds with O-6 substituted and those for **6** for the others. [c] The coupling constants reported by Padrón and Vásquez,[3b] 4.7 and 3.4 Hz, appear to be wrong and yield very different populations. [d] The populations reported[2] for this compound were incorrect; application of eqs 1−3 using the reported[2] coupling constants gave results different than those reported.[2]

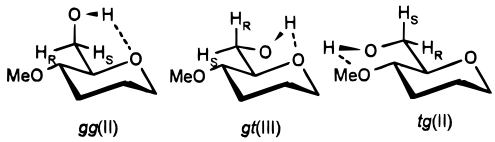

Figure 7. C5−C6 rotameric conformations in which OH-6 can act as an intramolecular hydrogen bond donor.

amount of the *gt* rotamer increased from 18% to 40%, that of the *tg* rotamer decreased from 9% to negligible, and that of the *gg* rotamer decreased from 73% to 60%. It should be noted that the values in the most polar environments are virtually identical to the rotamer populations for **2a**, where the group on C-6 cannot be a hydrogen bond donor. The presence of significant amounts of the *tg* rotamer in nonpolar solvents can only be due to intramolecular hydrogen bonding of OH-6 to O-4 because no other factor would favor this conformer under nonpolar conditions.

The *tg* population, if dependent on intramolecular hydrogen bonding, should be best correlated to β_{kt}, the hydrogen bond acceptor parameter.[63] In fact, the amount of *tg* rotamer shows a much better correlation to the Kirkwood function (ϵ_k, see eq 4), which was developed for examining solvent effects on neutral polar molecules.[68]

$$\epsilon_K = \frac{\epsilon - 1}{2\epsilon + 1} \tag{4}$$

Correlations of the hydroxyl NMR parameters to solvent parameters are informative with respect to the extent of intramolecular hydrogen bonding. As expected, there is a very good ($R^2 = 0.985$) correlation between the chemical shift of the hydroxyl proton and β_{kt}. The populations of rotamers II and III (see Figures 5 and 7) correlate very well with ϵ_k, but this could be a product of the small data set and the asymptotic values of ϵ_k for polar solvents. The population of rotamer I shows no correlation to any of the solvent parameters.

The three rotamers of the OH group each have different potentials to hydrogen bond. Rotamer I cannot participate in any intramolecular hydrogen bonding (see Figures 5 and 7). This rotamer should be most favored when intermolecular bonding dominates. Rotamers II and III are capable of intramolecular or intermolecular hydrogen bonding depending on the geometry around the C5−C6 bond (see Figure 7). In the *gg* and *tg* rotamers, intramolecular hydrogen bonds can form in hydroxyl rotamer II from OH6 to O5 and O4, respectively. In hydroxyl rotamer III, OH6 can hydrogen bond to the ring oxygen (O5) in the *gt* conformation. Increases in solvent polarity bring about decreases in the populations of the *tg* and *gg* populations and corresponding decreases in the population of rotamer II and increases in the population of rotamer I. These

(68) Chastrette, M.; Rajzmann, M.; Chanon, M.; Purcell, K. F. *J. Am. Chem. Soc.* **1985**, *107*, 1−11.

results are consistent with the conclusion that intramolecular hydrogen bonding occurred in these rotamers in nonpolar solvents.

The infrared spectra of compound **6** (see Figure 6) support this conclusion. The very broad peak in the hydrogen-bonded O−H stretching region of **6** in hexane indicates that there is more than one type of intramolecular hydrogen bond present.

The observed changes in rotamer populations for **6** as solvent polarity increases are most likely due to gradual weakening of the intramolecular hydrogen bonds. The population trends in polar solvents are due to the rotamer populations returning to their non-hydrogen-bonded population levels. The rotamer populations in water-d_2 are almost identical to those in the permethylated derivative **2a**, where no intramolecular hydrogen bonding can occur. These results are contrary to what has been predicted based on the calculated behavior of 2-(hydroxymethyl)- and 2-(methoxymethyl)tetrahydropyran.[29]

The small population of the hydrogen-bonded *tg* rotamer is in marked contrast to the results of Beeson et al.[34] on (1*S*,2*R*,4*S*)-4-*tert*-butyl-2-(hydroxymethyl)-1-methoxycyclohexane (**7**). This

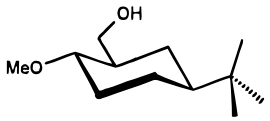

7

compound was present in chloroform as a rotameric mixture of which the hydrogen-bonded *tg* rotamer constituted 74% of the total, whereas solutions of the corresponding 2-methoxymethyl analogue contained none of the *tg* rotamer.[34] In comparison, the *tg* population in **6** is negligible in chloroform, presumably because the other rotamers are favored by reduced steric repulsion due to the replacement of a CH_2 by an oxygen atom, by the gauche effect, and by hydrogen bonding of OH-6 to O-5 discussed previously.

As solvent polarity increases, the population of the *gg* rotamer of **6** decreases, while that of the *gt* rotamer increases. This change probably reflects the decreasing amount of hydrogen bonding with increased solvent polarity. For **6**, calculations with MM394 indicate that the dipole moments of the *gg*, *gt*, and *tg* rotamers are 1.67, 2.16, and 2.98 D if the C5−C6−O6−H conformation is anti, the most stable arrangement for **2a**. However, for **6**, the most stable arrangements at the default dielectric constant has the C5−C6−O6−H conformations gauche to allow hydrogen bonding and in this arrangement, the rotamer dipole moments are calculated to be 2.84, 3.15, and 2.75 D, respectively. The O5−C5−C6−O5 torsional angle in this latter arrangement is calculated to be closer to gauche in the *gg*, −64.7° versus +68.1°, and the calculation at a larger dielectric constant, 30, changes the angle more for the *gg* rotamer, to −67.5° versus +69.4°. These values suggest that hydrogen bonding is somewhat stronger in the *gg* than the *gt* rotamer, and that, combined with the greater polarity of the latter (larger dipole moments for both OH rotamers) explains the change in populations.

There is an interesting trend relating the relative populations of the *gg* and *gt* rotamers to the structure of the substituent at C4 (see Table 8) that only became apparent when the original data[2] was reanalyzed with the better limiting coupling constants derived here and combined with that for the new compounds considered here. Now, it can be seen that α-D-glucopyranose derivatives in water with a free hydroxyl group at C4 (first four entries in Table 8) have the *gt* rotamer population greater than or equal to that of the *gg* rotamer, whereas the gg rotamer is more populated when O4 is methylated (compounds **2a** and **6**). Neither steric effects nor hydrogen bonding can influence this ratio which must be caused either by electronic factors or by disruption of interactions with solvent.

Other substituents on C-4 also affect this ratio as listed in Table 4. The 4-deoxy and 4-amino-4-deoxy derivatives have larger relative *gt* populations, while derivatives with 4-thio and 4-ammonium groups give larger relative *gg* populations. The increases in the population of the *tg* rotamer for the 4-deoxy and 4-ammonio-4-deoxy derivatives are caused by removal of the 1,3-repulsion and intramolecular hydrogen bonding, respectively, as previously discussed.[2]

Understanding of the solvation of carbohydrates is gradually increasing as a result of intense current interest. Solvation has been discussed in terms of two contributions: one is the polarization effect on the intrinsic stability of the molecule and the other is the direct solvent−solute interactions that include hydrogen bonding.[69] Both factors could influence hydroxymethyl rotamer populations. The equal rotamer populations for **2a** and **6** in water suggest that hydrogen bond donation of OH-6 to water is not important in solvation of these molecules or possibly that electronic factors of methyl substitution in **6** cancel hydrogen-bond donation in **2a**. However, the polarization effect of solvent on the intrinsic stability of the rotamers should be fairly similar for **2a** and **6**, suggesting that this is the primary way that solvation affects rotamer populations, consistent with the calculations of Barrows et al.[1]

Another view of solvation of carbohydrates in water is that the process depends on how well the carbohydrate molecule fits into the three-dimensional hydrogen bonding network of water. Particular carbohydrates that have pairs of oxygen atoms the same distance apart as the distance between the oxygen atoms of water are solvated better.[70] The 1,3-diaxially related pair of oxygen atoms in at C-2 and C-4 in talopyranose derivatives are postulated to fit into the structure of water particularly well.[70] However, O-4 and O-6 of glucopyranose are the same distance apart if the hydroxymethyl group is in the *tg* rotamer, suggesting that this rotamer should be particularly favored in water if O−O distance is the only factor. The absence of a preference for this rotamer indicates that factors other than matching water's OO separation distance are more important, consistent with contributions from a number of factors.[69b]

Solvent Effects on the H6R−H6S Chemical Shift Difference. For almost all glucose derivatives, the signal of H6S appears at a higher frequency than that of H6R. For compound **2a**, in all solvents other than water-d_2, this chemical shift order is reversed. Interestingly, for methyl 2,3,4-tri-*O*-[$^2H_3$]methyl-α-D-glucopyranoside (**6**) and 6-*O*-methyl-α-D-glucose,[2] the H6 signals have the normal chemical shift order for glucose derivatives. Thus, the chemical shift reversal in **2a** must be a substituent effect that occurs only when both O6 *and* O4 are substituted. A study of acetylated and benzoylated carbohydrates in chloroform-*d* by Rao and Perlin showed a similar chemical shift exchange which occurred only when both O6 *and* O4 were acetylated, but the analogous benzoylated deriva-

(69) (a) Ma, B.; Schaefer, H. F., III; Allinger, N. L. *J. Am. Chem. Soc.* **1998**, *120*, 3411−3422. (b) Giesen, D. J.; Hawkins, G. D.; Liotard, D. A.; Cramer, C. J.; Truhlar, D. G. *Theor. Chem. Acc.* **1997**, *98*, 85−109.

(70) (a) Galema, S. A.; Blandamer, M. J.; Engberts, J. B. F. N. *J. Am. Chem. Soc.* **1990**, *112*, 9665−9666. (b) Galema, S. A.; Høiland, H. *J. Phys. Chem.* **1991**, *95*, 5321−5326. (c) Galema, S. A.; Blandamer, M. J.; Engberts, J. B. F. N. *J. Org. Chem.* **1992**, *57*, 1995−2001. (d) Galema, S. A.; Engberts, J. B. F. N. *J. Phys. Chem.* **1993**, *97*, 6885−6889. (e) Galema, S. A.; Howard, E.; Engberts, J. B. F. N.; Grigera, J. R. *Carbohydr. Res.* **1994**, *265*, 215−225.

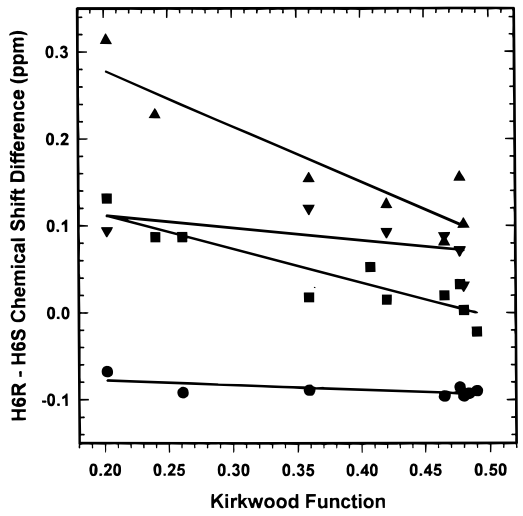

Figure 8. Plots of the chemical shift difference between H6R and H6S against the Kirkwood function, eq 4: (▲) methyl 2,3,4,6-tetra-*O*-acetyl-α-D-glucopyranoside (**8**); (▼) methyl 2,3,4,6-tetra-*O*-benzoyl-α-D-glucopyranoside (**9**); (■) methyl 2,3,4,6-tetra-*O*-[$^2H_3$]methyl-α-D-glucopyranoside (**2a**); (●) methyl 2,3,4-tri-*O*-[$^2H_3$]methyl-α-D-glucopyranoside (**6**).

tives did not show the chemical shift reversal.[71] The results were interpreted as being the result of the magnetic anisotropy of the acetyl groups on O6 and O4.

To evaluate the relative importance of solvent effects and anisotropy on these chemical shift effects, the ^{1}H NMR spectra of methyl 2,3,4,6-tetra-*O*-acetyl-α-D-glucopyranoside (**8**) and methyl 2,3,4,6-tetra-*O*-benzoyl-α-D-glucopyranoside (**9**) were recorded in a number of solvents and the H6R−H6S chemical shift differences were determined. As previously observed[71] for solutions in chloroform-*d*, the signal of H6R appeared at a greater frequency than that of H6S in all solvents for **8**. Surprisingly, the signals of H6R for **9** also appeared at a larger frequency in all solvents although the chemical shift differences were much smaller, contrary to the observation made for the *β*-analogue in chloroform-*d*.[71]

The H6R−H6S chemical shift differences for **2a**, **6**, **8**, and **9**

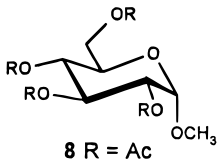

8 R = Ac
9 R = Bz

were correlated with the Kirkwood function (ϵ_K, eq 4), which has been used to examine solvent dielectric effects on neutral polar molecules (see Figure 8).[68,72] For **2a** and **8**, the H6S−H6R chemical shift difference depends on ϵ_K with slopes of −0.39 and −0.64 ppm, while for **6** and **9**, the chemical shift differences are almost solvent independent. For **2a**, the chemical shift reversal in water-d_2 is caused by the change in solvent polarity. Regression analysis indicates that the signal of H6S moves to a higher frequency as solvent polarity increases while that of H6R remains fixed (3.52 ± 0.09 ppm). When the solvent polarity reaches its maximum in water-d_2, H6S has shifted beyond H6R to give the chemical shift reversal (see Figure 8).

We believe that the solvent effect is a result of H6S being present on the α face of the glucose molecule in both of the dominant rotamers (*gg* and *gt*). Its relatively fixed location means that its solvation environment is relatively unchanging, and thus solvent effects on its chemical shift, such as polar deshielding effects,[73] are observed. The H6R proton is present on the α and *β* faces in the *gg* and *gt* rotamers, respectively, and thus, its solvation environment varies resulting in small chemical shift effects. This hypothesis is supported by the results for the galactose derivatives where both protons shift from the α to *β* faces and there is no evidence that either chemical shift is affected significantly by changes in solvent.[6] A similar mechanism would apply to the peracetylated case.[71] The fact that the feature is not observed for larger substituents such as benzoyl groups is due to perturbation of the solvent shell caused by the large nonpolar phenyl ring. In these situations, H6S and H6R have similar solvent effects and no reversal is observed.

Unlike compound **2a**, for **6,** there was no relationship between solvent polarity and the chemical shift difference of H6R and H6S. This result is consistent with the proposed mechanism presented above. For compound **6** and for other glucopyranose derivatives with OH-6 free, the hydroxyl group has a different solvation shell in different rotamers. Thus, despite the fact that H6S spends most of its time on the α side of the molecule as do **2a**, **7**, and **8**, the solvation shell changes as the rotamers interconvert and the chemical shift of H6S is no more sensitive to solvent than that of H6R.

Conclusions

The solvent dependence of the population of the hydroxymethyl rotamers of D-glucopyranoses has been determined by examination of two derivatives through analysis of $^3J_{H5,H6R}$ and $^3J_{H5,H6S}$ values and by consideration of evidence for hydrogen bonding through infrared spectroscopy and $^3J_{H,OH}$ values. The application of nonstaggered geometries from MM3 calculations for the derivation of rotamer coupling constants rather than assuming perfect staggering resulted in improved values of rotamer populations. Vibrational averaging based on a Boltzmann distribution of populations of conformations in each rotamer potential energy well did not improve the calculated populations further.

Unlike galactose derivatives, when O-6 is substituted, glucose rotamer equilibria are independent of solvent polarity. When O-6 is unsubstituted, there are changes in rotamer population as solvent polarity increases; however, once the solvent is of sufficiently high polarity, intramolecular hydrogen bonding ceases to be significant and the rotamer populations are identical to the populations when hydrogen bonding is not structurally possible. Thus, hydroxymethyl rotational preferences in water are not affected by hydrogen bond donation of OH-6 to water.

It has been shown through infrared and ^{1}H NMR analysis that significant intramolecular hydrogen bonding takes place in all rotamers in nonpolar solvents and that intramolecular hydrogen bonding is present (although much weakened) in solvents as polar as acetonitrile.

The absence of a solvent effect on the relative populations of the *gt* and *gg* rotamers for fully methylated derivative **2a** must mean that both rotamers are stabilized equally as polarity increases. The observed stabilization of the *tg* rotamer from negligible to just observable as polarity increases is probably

(71) Rao, V. S.; Perlin, A. S. *Can. J. Chem.* **1983**, *61*, 2688−2694.
(72) (a) Onsager, L. *J. Am. Chem. Soc.* **1936**, *58*, 1486−1493. (b) Abraham, R. J.; Cooper, M. A. *J. Chem. Soc. B* **1967**, 202−205. (c) Abraham, R. J.; Siverns, T. M. *J. Chem. Soc., Perkin Trans. 2* **1972**, 1587−1594.
(73) Buckingham, A. D.; Schaefer, T.; Schneider, W. G. *J. Chem. Phys.* **1960**, *32*, 1227−1233.
(74) Bock, K.; Thøgersen, H. *Ann. Rep. NMR Spectrosc.* **1982**, *13*, 1−57.

due to reduced electrostatic repulsions between O-4 and O-6 and favorable solvent−solute interaction because this rotamer has the largest dipole moment. In nonpolar solvents, the derivative with O-6 not methylated (**6**) had enhanced populations of the *tg* and *gg* rotamers that reverted to the same populations as present for **2a** when the polarity of the solvent was increased to that of water. The decrease of the population of the *tg* rotamer is due to the loss of intramolecular hydrogen bonding of OH-6 to O-4. The decrease in the population of the *gg* rotamer of **6** in favor of the *gt* rotamer as solvent polarity increases is ascribed to loss of its somewhat stronger hydrogen bonding and to the fact that the *gt* rotamer has a larger dipole moment.

The well-known[23] "reversed" chemical shift order of the two C6 protons of peracetylated glucopyranose derivatives was shown to be a result of solvent effects in addition to the accepted explanation, the anisotropy of the acetyl group. It was demonstrated that permethylated derivatives also give the chemical shift reversal as does methyl 2,3,4,6-tetra-*O*-benzoyl-α-D-glucopyranoside while the *β*-analogue does not. This solvent effect on the chemical shift difference is attributed to the fact that one of the two protons stays on the same side of the pyranose ring in the two populated rotamers while the other proton exchanges environments. If larger substituents are present on O-6 or if OH-6 is not substituted, the solvent cage is disrupted and the normal chemical shift order is observed.

Acknowledgment. T.B.G. and G.D.R. thank NSERC for a research grant and scholarships, respectively. We are grateful to Dr. M. Lumsden of ARMRC, Dr. Ian Burton of IMB, and Dr. J. R. Brisson of NRC for recording 400-, 500-, and 600-MHz NMR spectra, respectively. We are grateful to ARMRC for providing NMR time to record the other spectra. We thank Dr. A. S. Serianni for the generous gift of 4-[^{13}C]glucose.

Supporting Information Available: Tables containing the complete simulation results for the seven spin patterns (5 pages, print/PDF). See any current masthead page for ordering information and Web access instructions.

JA981958L